Letter Vol. 49, No. 16 / 15 August 2024 / Optics Letters 4717

Optics Letters

Perfect correlation vortices

Xiaofei Li,[1,2] Sajjad Bashiri,[1] Yuan Ma,[1] Chunhao Liang,[2] Yangjian Cai,[2] Sergey A. Ponomarenko,[1,3,*] and Zhiheng Xu[1]

[1]Department of Electrical and Computer Engineering, Dalhousie University, Halifax, Nova Scotia B3J 2X4, Canada
[2]Shandong Provincial Engineering and Technical Center of Light Manipulation and Shandong Provincial Key Laboratory of Optics and Photonic Devices, School of Physics and Electronics, Shandong Normal University, Jinan 250014, China
[3]Department of Physics and Atmospheric Science, Dalhousie University, Halifax, Nova Scotia B3H 4R2, Canada
*serpo@dal.ca

Received 13 May 2024; revised 3 July 2024; accepted 23 July 2024; posted 24 July 2024; published 15 August 2024

We introduce perfect correlation vortices and show that the degree of coherence of any such vortex at the source is nearly statistically homogeneous and independent of the topological charge of the vortex. We demonstrate that while slowly diffracting in free space, perfect correlation vortices maintain their "perfect" vortex structure; they are capable of preserving said structure even in strong atmospheric turbulence. Structural resilience to diffraction and turbulence sets the discovered perfect vortices apart from their coherent cousins and makes them suitable for free-space optical communications.

https://doi.org/10.1364/OL.529970

A coherent optical vortex (OV) features a helical phase with the electromagnetic energy circulating around a vortex core which is a line of zero field intensity and indeterminate (singular) phase [1,2]. The discovery of a fundamental link between any optical vortex and its orbital angular momentum [3] has triggered a flurry of research activity on OVs, culminating in numerous applications thereof to optical communications [4,5], optical trapping and tweezing [6,7], imaging [8], and even optical computing [9].

The phase singularity positions (intensity nulls) of a typical coherent OV strongly depend on the magnitude of the topological charge (TC) of the vortex [4,10]. However, the so-called perfect vortex beams were introduced [11] and actively explored [12,13] that alter this picture. The intensity profile of a realistic perfect vortex forms a thin ring of a radius nearly independent of the TC of the vortex [14]. Unfortunately, perfect vortices embedded into coherent optical fields quickly lose their vortex structure on free-space propagation.

At the same time, random optical fields endowed with OVs have also been explored theoretically [15–17] and experimentally [18–20]. As such partially coherent fields can carry OVs associated with their two-point spatial correlations [15–17], the term coherence vortices has been coined in Ref. [17]. Electromagnetic surface fields, such as random surface plasmon polaritons, can also be structured to possess correlation vortices [21]. In this context, reducing [22] or structuring [23] spatial coherence at the source was proposed to mitigate extreme susceptibility of perfect vortices to diffraction. Such perfect vortices wrapped into partially coherent fields remain intact over short propagation distances, but quickly succumb to diffraction afterward. Thus, realizing prefect vortices that are resilient against diffraction over any desired propagation distance remains an open challenge.

In this Letter, we address this challenge by introducing a class of perfect correlation vortices (PCVs) that maintain their perfect vortex correlation rings on free-space propagation. As a surprising bonus, the discovered PCVs are robust even against very strong atmospheric turbulence over moderate distances. In addition, the introduced PCVs are nearly immune to diffraction and are virtually statistically homogeneous in the low-coherence limit; their degree of coherence (DOC) is independent of the TC. All these remarkable features testify to the potential of such PCVs for free-space optical communications which we will explore in due course.

We start our search for PCVs by considering random sources endowed with OVs. The cross-spectral density of any bona fide structured random source can be represented in the form [24]

$$W_0(\mathbf{r}_1, \mathbf{r}_2) = \int d\mathbf{k}\, p(\mathbf{k}) \Psi^*(\mathbf{r}_1, \mathbf{k}) \Psi(\mathbf{r}_2, \mathbf{k}). \tag{1}$$

Let us take the nonnegative power spectrum $p(\mathbf{k})$ to be a Gaussian

$$p(\mathbf{k}) = p(k) \propto e^{-k^2\sigma_c^2}, \qquad k \geq 0, \tag{2}$$

and examine an infinite set of vortex carrying modes of the form

$$\Psi(\mathbf{r}, \mathbf{k}) = \Psi_m^{(k)}(\mathbf{r}) = \sqrt{k} J_m(kr) e^{-r^2/2w_0^2} e^{im\phi}. \tag{3}$$

Here $J_m(x)$ is a Bessel function of the first kind and order m. It follows from Eqs. (1) to (3) by inspection with the aid of the table integral [25]

$$\int_0^\infty dx x J_m(ax) J_m(bx) e^{-cx^2} \propto \exp\left(-\frac{a^2+b^2}{4c}\right) I_m\left(\frac{ab}{2c}\right), \tag{4}$$

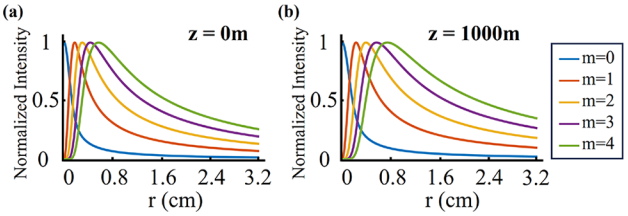

Fig. 1. (a) Intensity distribution and (b) its evolution on free-space propagation for PCVs of variable TC m. The parameters of the source are $w_0 = 10$ cm, $\sigma_c = 1$ mm, and $\lambda_0 = 532$ nm.

that the source cross-spectral density can be expressed, up to an irrelevant normalization constant, in a closed form as

$$W_0(\mathbf{r}_1, \mathbf{r}_2) \propto e^{im(\phi_2-\phi_1)} \exp\left(-\frac{r_1^2+r_2^2}{2w_0^2}\right) \times \exp\left(-\frac{r_1^2+r_2^2}{4\sigma_c^2}\right) I_m\left(\frac{r_1 r_2}{2\sigma_c^2}\right). \tag{5}$$

Here σ_c is related to the source coherence width as we will see shortly, and w_0 is a root mean square (rms) width of a Gaussian envelope. Further, $I_m(x)$ is a modified Bessel function of order m. We display the spatial intensity distribution $I(\mathbf{r}) = W(\mathbf{r}, \mathbf{r})$ of the source for variable m, which manifests intensity nulls on the optical axis for any $m \neq 0$, in Fig. 1(a). We choose the following parameters: $w_0 = 10$ cm, $\sigma_c = 1$ mm, and the carrier wavelength $\lambda_0 = 532$ nm. However, we are chiefly interested in the behavior of the DOC of the just presented source; the latter is defined as [26,27]

$$\mu_0(\mathbf{r}_1, \mathbf{r}_2) = \frac{W_0(\mathbf{r}_1, \mathbf{r}_2)}{\sqrt{W_0(\mathbf{r}_1, \mathbf{r}_1) W_0(\mathbf{r}_2, \mathbf{r}_2)}}. \tag{6}$$

It follows at once from Eqs. (5) and (6) that

$$\mu_0(\mathbf{r}_1, \mathbf{r}_2) = e^{im(\phi_2-\phi_1)} \frac{I_m[r_1 r_2/(2\sigma_c^2)]}{\sqrt{I_m[r_1^2/(2\sigma_c^2)] I_m[r_2^2/(2\sigma_c^2)]}}. \tag{7}$$

The first glance at Eqs. (5) and (7) might lead to the conclusion that the introduced sources are closely related to the previously reported [15] modified-Bessel-correlated ones. Indeed, the cross-spectral densities and hence the degrees of coherence of the two classes of sources have the same function form. Yet, careful inspection reveals that in the low-coherence regime, $\sigma_c \ll w_0$, the PCVs possess statistically homogeneous correlations of a perfect vortex type, while the modified-Bessel-correlated sources are statistically inhomogeneous in any parameter regime. Mathematically, this fact is reflected in very different representations of PCVs and modified-Bessel-correlated sources in terms of Bessel and Laguerre–Gaussian modes, respectively.

To demonstrate that the DOC of Eq. (7) describes a PCV, we focus on a nearly incoherent limit, such that

$$\sigma_c \ll \sigma_{\text{eff}} \ll w_0, \qquad \sigma_{\text{eff}} = \sqrt{\sigma_c w_0}. \tag{8}$$

Here σ_{eff} denotes a characteristic transverse spatial scale governing PCV diffraction, as we will see shortly. Next, introducing a dimensionless radial variable, $\bar{r} = r/\sigma_{\text{eff}}$, we can approximate $I_m(x) \simeq e^x/\sqrt{x}$ in the incoherent limit (8). It then readily follows from Eq. (7) that relative to any reference point $\mathbf{r}_0$, the source correlations are homogeneous, given by

$$\mu_0(\bar{\mathbf{r}}, \bar{\mathbf{r}}_0) \simeq e^{im(\phi-\phi_0)} \exp\left[-\frac{(\bar{r}-\bar{r}_0)^2}{4\delta_0^2}\right], \tag{9}$$

where $\bar{r}_0 = r_0/\sigma_{\text{eff}}$ and $\delta_0 = \sqrt{\sigma_c/w_0} \ll 1$ is a very narrow width of source correlations in dimensionless variables; in other words, the two-point correlations of the source field endowed with a helical wavefront are only significant over a very narrow circular ring, regardless of the topological charge of the vortex. Therefore, Eq. (9) describes a perfect correlation vortex. Note that $\bar{r}$ in the $\sqrt{x}$ factor in the asymptotic expansion of $I_m(x)$ can be replaced with $\bar{r}_0$ because $\sqrt{x}$ does not appreciably change over the ring width compared to e^x.

Next, we examine free-space evolution of PCVs. Using the vortex modes of Eq. (3), we can write for the cross-spectral density in any transverse plane, $z = const \geq 0$,

$$W(\mathbf{r}_1, \mathbf{r}_2, z) = \int_0^\infty dk e^{-k^2\sigma_c^2} \Psi_m^{(k)*}(\mathbf{r}_1, z) \Psi_m^{(k)}(\mathbf{r}_2, z), \tag{10}$$

where the mode evolution is governed, in paraxial approximation, by the following Fresnel transform:

$$\Psi_m^{(k)}(\mathbf{r}, z) = \left(\frac{k_0}{2\pi i z}\right) \int d\mathbf{r}' \Psi_m^{(k)}(\mathbf{r}', 0) \exp\left[\frac{ik_0(\mathbf{r}-\mathbf{r}')^2}{2z}\right]. \tag{11}$$

Here $k_0 = 2\pi/\lambda_0$. On substituting from Eqs. (3) and (11) into (10), we obtain, after somewhat lengthy algebra employing the integral (4), for the cross-spectral density the expression

$$W(\mathbf{r}_1, \mathbf{r}_2, z) \propto \frac{e^{im(\phi_2-\phi_1)}}{(1+z^2/L_d^2)} \exp\left[\frac{i(r_2^2-r_1^2)}{2(\sigma_c^2 L_R/z + w_0^2 z/L_R)}\right] \times \exp\left[-\frac{(r_1^2+r_2^2)}{2w_0^2(1+z^2/L_R^2)(1+z^2/L_d^2)}\right] \times \exp\left[-\frac{(r_1^2+r_2^2)}{4\sigma_c^2(1+z^2/L_d^2)}\right] I_m\left[\frac{r_1 r_2}{2\sigma_c^2(1+z^2/L_d^2)}\right]. \tag{12}$$

Here $L_R = k_0 w_0^2$ is a Rayleigh range associated with the envelope width w_0 and $L_d = k_0 \sigma_c w_0$ is a characteristic diffraction length of a PCV, which justifies our interpretation of σ_{eff} immediately following Eq. (8). Notice that in the chosen parameter regime, $L_d \ll L_R$.

A few instructive observations are in order at this point. First, it follows from Eq. (12) that the PCV field structure is invariant on free-space propagation, making PCVs a subclass of a larger class of vortex preserving partially coherent fields whose general theory was developed in [28]. Second, the spatial intensity distribution of the PCV, which we display in Fig. 1(b), is nearly diffraction free in the chosen parameter regime. At first glance, one might find this result surprising as the cross-spectral density of Eq. (12) is not of the form of a bump/dip atop of a statistically uniform background which would guarantee propagation invariance in general [29]. However, we can show that provided $\sigma_c \ll w_0$, the source cross-spectral density can be approximated, apart from a helical phase factor, by a product of a very wide Gaussian envelope and a uniform Gaussian correlation function of width σ_c. It follows that over distances of the order of $L_d \sim 1$ km, the field generated by such a source outside of the vortex core region behaves as a partially coherent plane wave, which is essentially immune to diffraction. We note also that the dependence of the diffraction length of PCVs on the product of their coherence width and soft aperture size is typical of enveloped diffraction-free random beams [30].

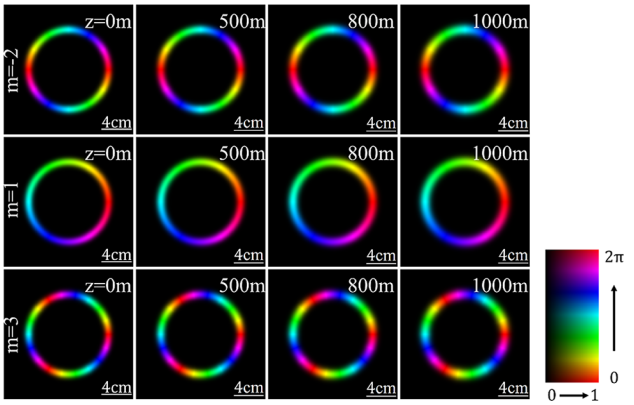

Fig. 2. Evolution of the magnitude and phase (hue) of the DOC of a PCV, given by Eq. (14), with the propagation distance. The source parameters are $w_0 = 10$ cm, $\sigma_c = 1$ mm, $r_0 = 2$ cm, and $\lambda_0 = 532$ nm.

Next, the DOC of a PCV in any transverse plane is defined as

$$\mu(\mathbf{r}_1, \mathbf{r}_2, z) = \frac{W(\mathbf{r}_1, \mathbf{r}_2, z)}{\sqrt{W(\mathbf{r}_1, \mathbf{r}_1, z) W(\mathbf{r}_2, \mathbf{r}_2, z)}}. \tag{13}$$

It follows at once from Eqs. (12) and (13) that

$$\mu_{\text{exact}}(\mathbf{r}, \mathbf{r}_0, z) = \frac{I_m\left[\frac{r r_0}{2\sigma_c^2(1+z^2/L_d^2)}\right] e^{im(\phi-\phi_0)}}{\sqrt{I_m\left[\frac{r^2}{2\sigma_c^2(1+z^2/L_d^2)}\right] I_m\left[\frac{r_0^2}{2\sigma_c^2(1+z^2/L_d^2)}\right]}}. \tag{14}$$

We exhibit the DOC evolution, obeying Eq. (14), over a kilometer-long distance in free space in Fig. 2; we show both the magnitude and phase evolution with z choosing the same parameters as before and the reference point to be at $r_0 = 2$ cm. We can infer from the figure that both the DOC magnitude and phase, shown with hue, remain nearly intact, thereby attesting to PCV robustness to diffraction.

We now derive a simple and elegant approximate expression for the PCV DOC, which is valid in any transverse plane $z \geq 0$, and demonstrate its accuracy. To this end, we infer from Eq. (12) that provided $z \lesssim L_d$, the vortex ring of the DOC remains narrow enough so that by approximating the modified Bessel function with an exponential, we obtain in dimensionless variables the expression

$$\mu(\bar{\mathbf{r}}, \bar{\mathbf{r}}_0, z) \simeq e^{im(\phi-\phi_0)} \exp\left[-\frac{(\bar{r}-\bar{r}_0)^2}{4\delta^2(z)}\right], \tag{15}$$

where

$$\delta(z) = \delta_0\sqrt{1 + z^2/L_d^2}, \tag{16}$$

is a width of the PCV ring at a distance z; Eq. (15) indicates that the PCV remains statistically homogeneous within the paraxial propagation regime. Equations (15) and (16) are the key result of this work; they provide a universal, as expressed in dimensionless variables, and application friendly description of field correlations of an ideal PCV. To verify the accuracy of this approximation, we display the magnitude of the DOC obtained with the aid of Eq. (14) and that given by the approximate equation, Eq. (15) in Fig. 3. The top two rows juxtapose the exact and approximate $|\mu|$ for a moderate value of the TC $m = 3$, while the bottom two rows do the same for large m, $m = 180$.

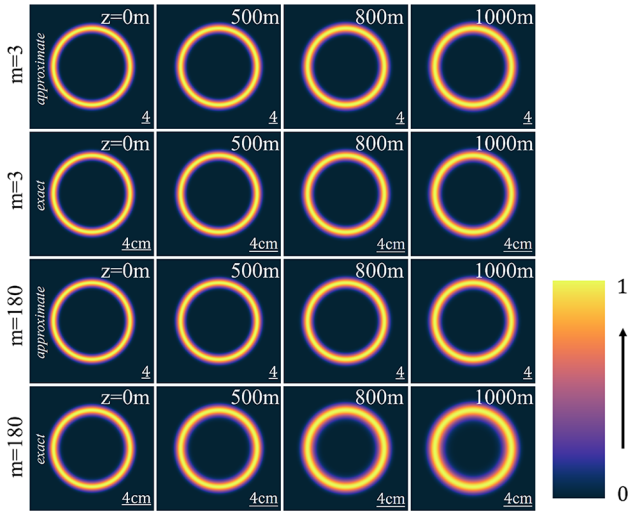

Fig. 3. Comparing the magnitude of DOC evolution obtained from the exact expression, Eq. (14) and the corresponding Gaussian approximation, Eq. (15) with z over a kilometer-long stretch of free space. The source parameters are $w_0 = 10$ cm, $\sigma_c = 1$ mm, $r_0 = 2$ cm, and $\lambda_0 = 532$ nm.

We can readily infer from the figure that there is an excellent agreement between the exact and approximate expressions for $|\mu|$ with moderate TCs. We also observe in the figure that as the magnitude of the TC increases, the ring radius, but not the circular shape, starts deviating from that of the ideal PCV; the deviation becomes progressively noticeable as the PCV propagates farther away from the source. To assess the discrepancy quantitatively, we evaluate the (dimensionless) rms width Δ_m of the PCV field correlations which we define by the expression

$$\Delta_m^2(z) = \frac{\int_0^\infty d\bar{r} \int_0^\infty d\bar{r}_0 |\mu_{\text{exact}}(\bar{r}, \bar{r}_0)|^2 (\bar{r}-\bar{r}_0)^2}{\int_0^\infty d\bar{r} \int_0^\infty d\bar{r}_0 |\mu_{\text{exact}}(\bar{r}, \bar{r}_0)|^2}, \tag{17}$$

where we employed the exact DOC given by Eq. (14) and expressed in dimensionless variables. In Fig. 4, we compare thus defined Δ_m with δ, evaluated at the source for variable topological charge m. We also display δ and Δ_m for $m = 5$ as functions of the propagation distance z. It follows from Fig. 4(a) that the correlation width does increase with m and the ideal PCV expression, Eq. (16), yields an appreciable error, around 30% for m corresponding to a double digit number. At the same time, Fig. 4 (b) attests to the fact that the magnitudes of Δ_m and δ remain quite close over substantial distances as long as m is not too large.

Finally, we demonstrate that the vortex ring structure of the discovered PCVs can be robust even against strong atmospheric turbulence, at least, over relatively short distances. To this end, we display in Fig. 5 the results of our numerical simulations for the evolution of the magnitude of the DOC of the PCV field through atmospheric turbulence with the structure constant such that $C_n^2 = 10^{-13}$ m$^{-2/3}$, which allows us to classify such turbulence as strong [31]. We employ a random phase screen method; the details of our numerical procedure can be found in [32]. We infer from the figure that, remarkably, the main correlation ring of the PCV with $m = 1, -2, 3$, which we have considered here, survives the turbulence rather well; similar results hold for PCVs with other TCs. At the same time, the contrast between the dark areas inside and outside the vortex ring on the one hand,

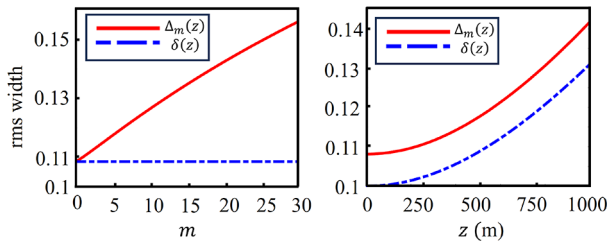

Fig. 4. Comparison of the widths of an ideal PCV ring δ with that determined from the rms width of the exact DOC profile Δ_m. Left: Δ_m and δ as functions of m at $z = 500$ m. Right: δ and Δ_m as functions of the propagation distance z for $m = 5$.

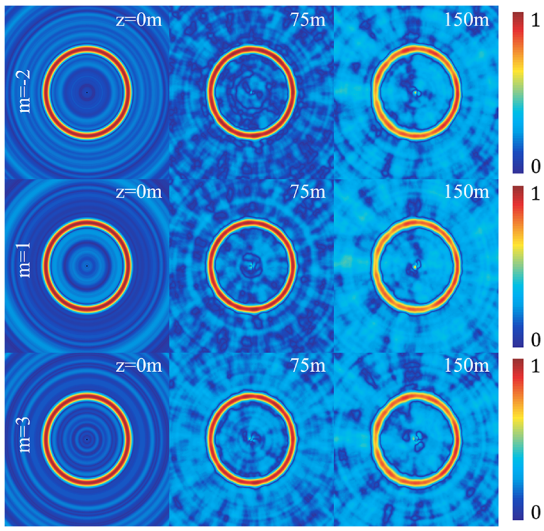

Fig. 5. Evolution of the magnitude of PCV DOC through a 150 m long stretch of the turbulence atmosphere with the structure constant C_n, $C_n^2 = 10^{-13}$ m$^{-2/3}$. The source parameters are $w_0 = 10$ cm, $\sigma_c = 1$ mm, and $\lambda_0 = 532$ nm. The reference point corresponds to $r_0 = 2$ cm and $\phi_0 = 0$.

and the bright area within the ring on the other hand, diminishes due to turbulence. We note, though, that the additional pseudo-rings, visible in all panels, are an artifact of our using a MATLAB random number generator. We also verified numerically that the orbital angular momentum spectrum of any PCV in Fig. 5 is sharply peaked around the corresponding topological charge over the entire propagation stretch. Finally, we notice that the axial symmetry of the magnitude of the source DOC breaks down on PCV propagation through atmospheric turbulence which becomes evident if we compare panels at $z = 0$ with those at $z = 75$ m, or $z = 150$ m. The resilience of the PCV ring to atmospheric turbulence is most consequential for the PCV potential for free-space optical communications.

In conclusion, we have introduced a class of random vortices, perfect correlation vortices, with the DOC at the source manifesting a thin ring of the radius and thickness independent of the topological charge of the vortex. The discovered PCVs are nearly statistically homogeneous across the source and remain so on paraxial propagation in free space. Thus, unlike their fully coherent counterparts, PCVs can maintain their vortex structure in free space essentially indefinitely. In addition, PCVs are resilient to even strong atmospheric turbulence, albeit over sufficiently short distances. We have derived an elegant, closed-form analytical expression for the degree of coherence of a perfect correlation vortex in any transverse plane. We anticipate the discovered vortices to facilitate free-space optical communications, among other potential applications.

Funding. National Key Research and Development Program of China (2022YFA1404800, 2019YFA0705000); National Natural Science Foundation of China (12192254, 92250304, 12374311); Natural Sciences and Engineering Research Council of Canada (RGPIN-2018-05497).

Disclosures. The authors declare no conflicts of interest.

Data availability. Data underlying the results presented in this Letter are not publicly available but may be obtained from the authors upon reasonable request.

REFERENCES

1. M. Soskin and M. Vasnetsov, in *Progress in Optics*, Vol. 42 (Elseveier, 2001), pp. 219–276.
2. M. R. Dennis, K. O'holleran, and M. J. Padgett, in *Progress in Optics*, Vol. 53 (Elsevier, 2009), pp. 293–363.
3. L. Allen, M. W. Beijersbergen, R. Spreeuw, *et al.*, Phys. Rev. A **45**, 8185 (1992).
4. A. M. Yao and M. J. Padgett, Adv. Opt. Photonics **3**, 161 (2011).
5. J. Wang, J.-Y. Yang, I. M. Fazal, *et al.*, Nat. Photonics **6**, 488 (2012).
6. K. Gahagan and G. Swartzlander, Opt. Lett. **21**, 827 (1996).
7. J. Chen, C. Wan, and Q. Zhan, Sci. Bull. **63**, 54 (2018).
8. J. H. Lee, G. Foo, E. G. Johnson, *et al.*, Phys. Rev. Lett. **97**, 053901 (2006).
9. X. Li, X. Liu, Q. Wu, *et al.*, APL Photonics **9**, 046107 (2024).
10. E. Karimi, G. Zito, B. Piccirillo, *et al.*, Opt. Lett. **32**, 3053 (2007).
11. A. S. Ostrovsky, C. Rickenstorff-Parrao, and V. Arrizón, Opt. Lett. **38**, 534 (2013).
12. J. García-García, C. Rickenstorff-Parrao, R. Ramos-García, *et al.*, Opt. Lett. **39**, 5305 (2014).
13. P. Vaity and L. Rusch, Opt. Lett. **40**, 597 (2015).
14. J. Pinnell, V. Rodríguez-Fajardo, and A. Forbes, Opt. Lett. **44**, 5614 (2019).
15. S. A. Ponomarenko, J. Opt. Soc. Am. A **18**, 150 (2001).
16. I. D. Maleev, D. M. Palacios, A. S. Marathay, *et al.*, J. Opt. Soc. Am. B **21**, 1895 (2004).
17. G. Gbur, T. D. Visser, and E. Wolf, J. Opt. A: Pure Appl. Opt. **6**, S239 (2004).
18. G. V. Bogatyryova, C. V. Fel'de, P. V. Polyanskii, *et al.*, Opt. Lett. **28**, 878 (2003).
19. D. Palacios, I. Maleev, A. Marathay, *et al.*, Phys. Rev. Lett. **92**, 143905 (2004).
20. J. Yu, X. Zhu, F. Wang, *et al.*, Prog. Quantum Electron. **91-92**, 100486 (2023).
21. Y. Chen, A. Norrman, S. A. Ponomarenko, *et al.*, Phys. Rev. A **100**, 053833 (2019).
22. X. Li, H. Wei, T. D. Visser, *et al.*, Appl. Phys. Lett. **119**, 171108 (2021).
23. X. Liu, Y. Wu, K. Zhu, *et al.*, J. Appl. Phys. **135**, 163106 (2024).
24. F. Gori and M. Santarsiero, Opt. Lett. **32**, 3531 (2007).
25. I. S. Gradshteyn and I. M. Ryzhik, in *Table of Integrals, Series, and Products* (Academic Press, 2014).
26. L. Mandel and E. Wolf, in *Optical Coherence and Quantum Optics* (Cambridge University Press, 1995).
27. S. A. Ponomarenko and E. Wolf, Opt. Commun. **170**, 1 (1999).
28. Z. Xu, X. Li, X. Liu, *et al.*, Opt. Express **28**, 8475 (2020).
29. S. A. Ponomarenko, W. Huang, and M. Cada, Opt. Lett. **32**, 2508 (2007).
30. M. Hajati, V. Sieben, and S. A. Ponomarenko, Opt. Lett. **46**, 3961 (2021).
31. L. C. Andrews and R. L. Phillips, in *Laser Beam Propagation Through Random Media*, 4th ed. (SPIE, 2005).
32. Z. Xu, X. Liu, Y. Cai, *et al.*, J. Opt. Soc. Am. A **39**, C51 (2022).